frontiers | Frontiers in Veterinary Science

TYPE Original Research
PUBLISHED 02 September 2022
DOI 10.3389/fvets.2022.930608

OPEN ACCESS

EDITED BY
Maxim C-J. Cheeran,
University of Minnesota, United States

REVIEWED BY
Hiroshi Asakura,
National Institute of Health Sciences (NIHS), Japan
Naveen Kumar,
ICAR-National Institute of High Security Animal Diseases (ICAR-NIHSAD), India

*CORRESPONDENCE
Jung-Eun Park
jepark@cnu.ac.kr
Tae-Won Kim
taewonkim@cnu.ac.kr

SPECIALTY SECTION
This article was submitted to Veterinary Infectious Diseases, a section of the journal Frontiers in Veterinary Science

RECEIVED 28 April 2022
ACCEPTED 16 August 2022
PUBLISHED 02 September 2022

CITATION
Kim J, Jo S, Choi Y, Kim T-W and Park J-E (2022) Chestnut inner shell extract inhibits viral entry of porcine epidemic diarrhea virus and other coronaviruses *in vitro*. *Front. Vet. Sci.* 9:930608. doi: 10.3389/fvets.2022.930608

Chestnut inner shell extract inhibits viral entry of porcine epidemic diarrhea virus and other coronaviruses *in vitro*

Jinman Kim[1], Sohee Jo[1], Yeojin Choi[1], Tae-Won Kim[1,2]* and Jung-Eun Park[1,2]*

[1]College of Veterinary Medicine, Chungnam National University, Daejeon, South Korea, [2]Research Institute of Veterinary Medicine, Chungnam National University, Daejeon, South Korea

Porcine epidemic diarrhea virus (PEDV) is a coronavirus that causes acute diarrhea in suckling piglets. Although vaccines are able to reduce the incidence of PEDV infection, outbreaks of PEDV continue to be reported worldwide and cause serious economic losses in the swine industry. To identify novel antiviral sources, we identified the chestnut (*Castanea crenata*) inner shell (CIS) as a natural material with activity against PEDV infection *in vitro*. The ethanol fractions of CIS extracts potently inhibited PEDV infection with an IC90 of 30 μg/ml. Further investigation of the virus lifecycle demonstrated that CIS extract particularly targeted the early stages of PEDV infection by blocking viral attachment and membrane fusion at rates of 80∼90%. In addition, CIS extract addition reduced the viral entry of other members of the *Coronaviridae* family. Our data demonstrated that CIS extract inhibited PEDV infection by blocking cell entry *in vitro* and suggest that CIS extract is a new prophylactic and therapeutic agent against PEDV and other coronavirus infections.

KEYWORDS

chestnut inner shell, porcine epidemic diarrhea (PED), coronavirus, entry, inhibition

Introduction

Porcine epidemic diarrhea virus (PEDV) infection is a highly contagious enteric disease associated with acute watery diarrhea, vomiting, and dehydration in suckling piglets (1–3). PEDV was first identified in 1978 in Europe (4) and then spread to Asian countries (5). A pathogenic variant of PEDV with higher morbidity and mortality emerged in China in 2010, and since then, this variant has been reported in many countries in Europe, Asia, and the United States and has caused considerable economic losses (6–8). Although commercial vaccines partially protect against the disease, PEDV endemic has persisted in many countries. Moreover, PEDV can persist in weaned piglets and sows with mild clinical symptoms (9, 10). Thus, novel effective prophylactics and/or therapeutics need to be developed.

Natural products are an essential source of novel chemical compounds with unique pharmacological activities. Among them, chestnut (*Castanea crenata*) inner shell extract (CISE) has benefits such as anti-wrinkling and whitening effects and anti-obesity,

hepatoprotective, and antioxidant activities (11–17). These effects are considered to be mediated by the active components scopoletin and scoparone, but the content of these compounds in CISE is unknown (12, 14, 15, 17). Gallic acid and ellagic acid are the most abundant components in CISE (18, 19). The antiviral activity of gallic acid and ellagic acid has been shown for many viruses, such as human influenza virus A, human rhinovirus, Ebola virus, and human papilloma virus (20–23). These studies indicate the possibility that CISE may block viral infection, but the antiviral effect of CISE has not yet been reported.

In the present study, we first determined the antiviral activity of CISE on cells infected with PEDV. CISE inhibited viral entry by blocking virus–cell binding and membrane fusion and exhibited antiviral activity against other CoVs, which suggests that it has excellent potential as a natural broad-spectrum anti-coronavirus product.

Materials and methods

Cells

HEK293T (ATCC® CRL-3216™), Huh7 (KTCC KCLM60104), and Vero (ATCC® CCL-81™) cells were maintained in Dulbecco's modified Eagle's medium (DMEM) supplemented with 10% fetal bovine serum, 100 IU/ml penicillin, and 100 μg/ml streptomycin.

Plasmids

Plasmids encoding pNL4.3-Luc.R-E-, vesicular stomatitis virus glycoprotein (VSV G), severe acute respiratory syndrome (SARS)-CoV spike (S) and Middle East respiratory syndrome (MERS)-CoV S were obtained from Tom Gallagher (Loyola University Chicago, Maywood, IL, USA). Plasmids encoding SARS-CoV-2 S with a C-terminal C9 tag were synthesized by GenScript and cloned into the pcDNA3.1 (+) vector (Invitrogen) using *EcoRI/NotI* sites.

Virus propagation and titration

PEDV strain SM98 was propagated in Vero cells as described previously (24). Briefly, Vero cells were washed twice with phosphate-buffered saline (PBS) and inoculated with PEDV at a multiplicity of infection (MOI) of 0.01. After 2 h, the inoculums were removed, and the cells were incubated in DMEM containing 10 μg/ml trypsin (Sigma–Aldrich) for 24 h.

The PEDV titers were determined by plaque assay. Vero cells were inoculated with 10-fold serially diluted virus. After 1 h at 37°C, the inoculums were aspirated, and the cells were maintained in minimum essential medium containing 0.6% agar and 10 μg/ml trypsin. After 2 days, the cells were stained with a crystal violet solution (Sigma–Aldrich).

Preparation of CISE

CISE was prepared according to a previous study (25). In brief, *Castanea crenata* (Shingongju Chestnut Agricultural Cooperative, Gong-ju, Korea) was peeled, and the chestnut inner shell was dried at 40°C for 3 days. The dried inner shell was ground to powder with a crusher, and the powder (300 g) was soaked in 70% ethanol (3 L) at room temperature for extraction. After 24 h of incubation, the aqueous layer was collected, and the extraction was repeated 3 times. The collected supernatant was concentrated with a rotary evaporator (Heidolph, Schwabach, Germany) at 40°C and freeze–dried with a HyperCOOL 3110 (Hanil Scientific Inc., Seoul, Korea). The lyophilized extract (40 g) was suspended in water (100 ml) and then subjected to conditioned Diaion HP-20 (Mitsubishi Chemical, Tokyo, Japan) open column (5 × 40 cm) chromatography. Elution was performed with distilled water (2 L) followed by ethanol (2 L). Each water and ethanol fraction was concentrated and freeze–dried, and the extraction yields for the water (CISE-DW) and ethanol (CISE-ET) fractions were 7.5 and 1.5%, respectively. The reproducibility of the CISE preparation was confirmed by additional extractions and HPLC analysis using raw materials from the same region and period.

High-performance liquid chromatography analysis

Serial dilutions of the reference standards gallic acid and ellagic acid were prepared in methanol and 10% DMSO in methanol, respectively. The sample peaks were confirmed by comparing the reference standard peak in terms of the retention time (RT) and consistency using an ultraviolet (UV) detector. The analysis was performed by HPLC coupled with a UV detector (1,260 Infinity II LC System, Agilent), and the chromatographic separation assay was performed with an Eclipse Plus C18 analytical column (Agilent, 150 × 2.6 mm, 3.5-μm particle size) according to a previous study (25). The mobile phase consisted of 0.1% formic acid in distilled water (A) and acetonitrile (B), the flow rate was 0.12 ml/min, and the linear gradient program was the following: 0–30 min (95–70% A), 30–57 min (70–5% A), and 57–70 min (5–95% A). The injection volume was 2 μl, and the wavelength was set to 275 nm.

Cell viability assay

Cell viability was determined by the MTT assay. A total of 1×10^4 cells per well were seeded into 96-well plates and incubated with CISE, CISE-ET, and CISE-DW at various

concentrations for 24 h. EX-cytox (Itsbio, Korea) was added to each well and incubated at 37°C for 1 h. The absorbance was measured using a microplate spectrophotometer at 450 nm.

In vitro antiviral assay

Vero cells grown in 12-well plates were washed with PBS and infected with PEDV at an MOI of 0.1 in the presence of various doses of CISE, CISE-ET, and CISE-DW at 37°C. At 2 h post-infection (hpi), the inoculums were removed, and the cells were maintained in DMEM containing various doses of CISE. At 24 hpi, the medium was removed, and the cells were freeze–thawed in serum-free medium (SFM). The virus infectivity was presented as a percentage of the virus titer in the treated group compared with that of the DMSO control group, and the 90% inhibitory concentration (IC90) was calculated.

For the time-of-addition experiment, Vero cells grown in 4-well plates were washed with PBS and infected with PEDV at an MOI of 1 for 2 h at 37°C. At 2 hpi, the virus inoculums

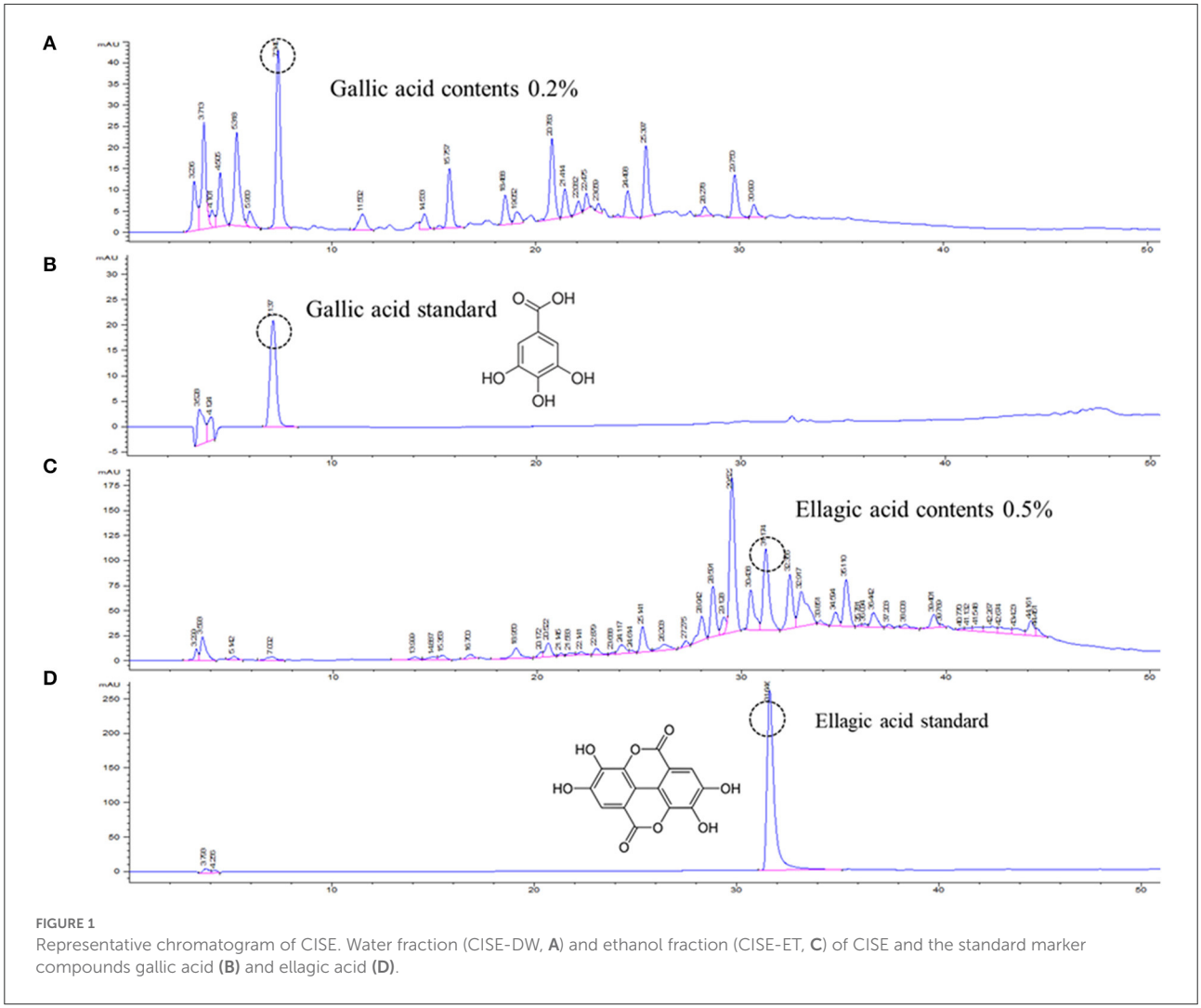

FIGURE 1
Representative chromatogram of CISE. Water fraction (CISE-DW, **A**) and ethanol fraction (CISE-ET, **C**) of CISE and the standard marker compounds gallic acid **(B)** and ellagic acid **(D)**.

TABLE 1 Regression equation with the LODs and LOQs of gallic acid and ellagic acid.

Compound	RT[a] (min)	UV (nm)	Regression equation	r^{2b}	LOD[c] (μg/ml)	LOQ[d] (μg/ml)
Gallic acid	7.1	275	y = 42.3x + 3.6	0.999	0.15	0.5
Ellagic acid	31.7	275	Y = 36.6x – 21.6	0.999	0.15	0.5

[a]RT, retention time; [b]r^2, correlation coefficient; [c]LOD, limit of detection; [d]LOQ, limit of quantitation.

10.3389/fvets.2022.930608

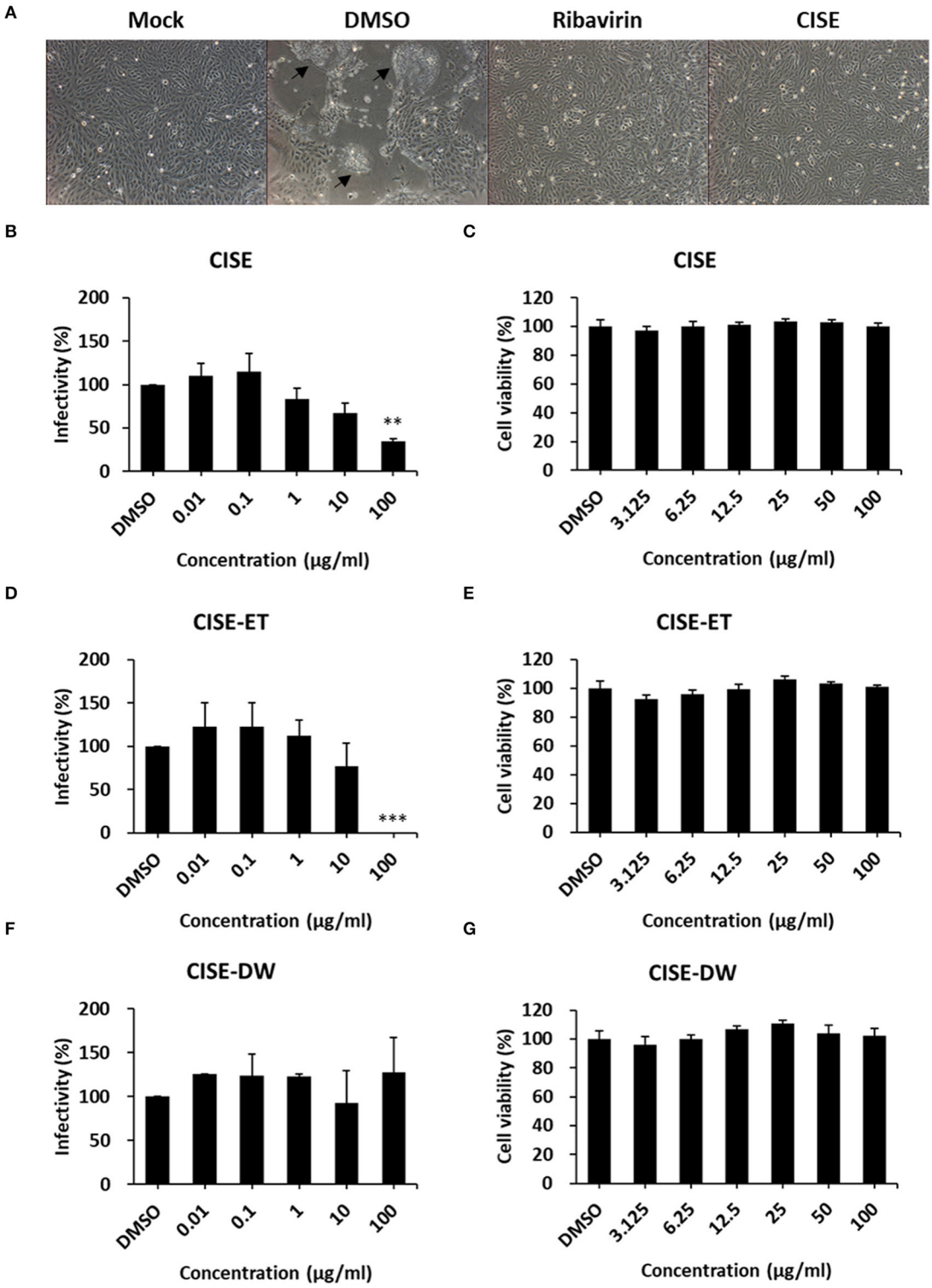

FIGURE 2
CISE inhibited PEDV infection in Vero cells. **(A)** Vero cells were infected with PEDV (MOI = 0.1) in the presence of CISE (50 μg/ml), ribavirin (50 μg/ml), or a DMSO control. At 24 hpi, a cytopathic effect (black arrow) was observed. **(B–G)** Vero cells were infected with PEDV (MOI = 0.1) in the presence of various concentrations of CISE **(B)**, CISE-ET **(D)**, or CISE-DW **(F)**. At 24 hpi, the virus titers were measured by plaque assay. Vero cells were incubated with various concentrations of CISE **(C)**, CISE-ET **(E)**, or CISE-DW **(G)** for 24 h, and the cell viability was then evaluated by the MTT assay. The antiviral activity and cell viability are expressed relative to those found for the DMSO control group. The error bars represent the SDs from the means ($n = 3$). $^{**}P < 0.01$; $^{***}P < 0.001$.

were removed, and 30 μg/ml CISE-ET was added at 0, 2, 4, and 6 hpi. At 10 hpi, the medium was removed, and the cells were freeze–thawed in SFM.

For the virus–cell binding experiment, Vero cells grown in 4-well plates were washed with PBS and infected with PEDV at an MOI of 1 with or without 30 μg/ml CISE-ET for 1 h at 4°C. At 1 hpi, the inoculums were removed, and the cells were maintained in SFM for 8 h.

For the cell pretreatment experiment, Vero cells grown in 4-well plates were washed with PBS and incubated with 30 μg/ml CISE-ET for 1 h at 37°C. After 1 h, the cells were washed with PBS and infected with PEDV at an MOI of 1 for 2 h at 37°C. At 2 hpi, the inoculums were removed, and the cells were maintained in SFM for 8 h.

For the virus pretreatment experiment, PEDV was incubated with or without 30 μg/ml CISE-ET for 1 h at 37°C. After 1 h, PEDV was diluted in SFM, and cells were infected with diluted PEDV at an MOI of 1 for 2 h at 37°C. At 2 hpi, the inoculums were removed, and the cells were maintained in SFM for 8 h.

For the virus–cell fusion experiment, Vero cells were infected with PEDV at an MOI of 1 for 1 h at 4°C. After 1 h, the cells were washed with PBS and treated with 30 μg/ml CISE-ET and/or 10 μg/ml trypsin for 2 h at 37°C. At 2 hpi, the inoculums were removed, and the cells were maintained in SFM for 8 h. In all the experiments, the virus titers were examined by plaque assay as described above.

Generation and transduction of pseudotyped viruses

HEK293T cells were transfected with plasmids encoding MERS-CoV S, SARS-CoV S, SARS-CoV-2 S or VSV G along with pNL4.3-Luc.R-E-. At 48 h post-transfection, the supernatants were collected, filtered through 0.45-μm syringe filters, and stored at −80°C until use.

For transduction, Huh7 cells were transduced with pseudotyped viruses in the presence of various concentrations of CISE or CISE-ET for 1 h at 37°C. At 48 h post-transduction, the cells were lysed in cell culture lysis buffer (Promega), and the luciferase levels were measured by the addition of Fluc substrate (Promega) and the use of a Veritas microplate luminometer (Turner BioSystems). The virus infectivity is presented as a percentage of luciferase activity of the treated group compared with that of the DMSO control group, and the 50% inhibitory concentration (IC50) was calculated.

Statistical analyses

All experiments were independently repeated at least two times. The data are presented as the means ± SDs. The statistical significance was calculated using the Holm–Sidak multiple Student's *t*-test procedure. A $P < 0.05$ was considered to indicate statistical significance.

Results

Preparation and characterization of CISE

Open column chromatography was performed to produce water and ethanol fractions, and a fingerprint chromatogram of the extract was obtained by HPLC analysis (Figure 1). Gallic acid and ellagic acid were analyzed as marker compounds of CISE-DW and CISE-ET, respectively. The linear regression analysis data for the standard compounds gallic acid and ellagic acid are provided in Table 1. CISE-DW was standardized with gallic acid, the content was ∼0.2% of CISE-DW, CISE-ET was standardized with ellagic acid, and the content was ∼0.5% of CISE-ET (Figure 1).

CISE-ET inhibited PEDV infection *in vitro*

To examine the PEDV antiviral activity of CISE, Vero cells were infected with PEDV in the presence or absence of

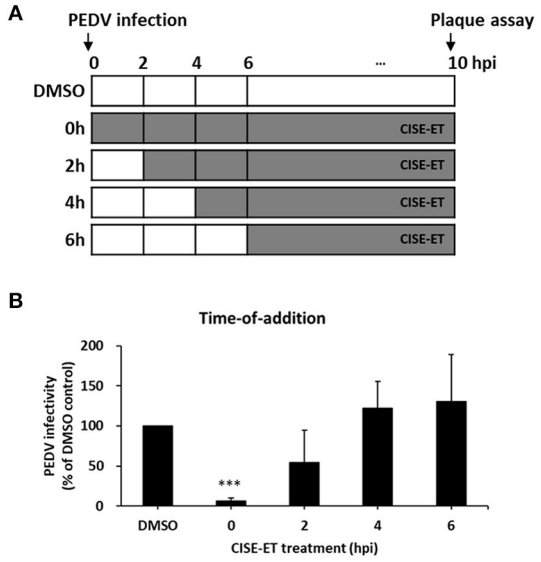

FIGURE 3
CISE-ET inhibited the early phase of PEDV infection. **(A)** Schematic of the time-of-addition experiments. Vero cells were infected with PEDV (MOI = 1), and 30 μg/ml CISE-ET was added at the indicated time points after virus infection. At 10 hpi, the virus titers were measured by plaque assay. **(B)** The viral infectivity is expressed relative to that obtained for the DMSO control group. The error bars represent the SDs from the means ($n = 3$). ***$P < 0.001$.

CISE, and the cytopathic effect and virus titers were evaluated. As shown in Figure 2A, PEDV-infected cells in the DMSO control group showed a significant cytopathic effect (cell–cell fusion) at 24 hpi. The PEDV-associated cytopathic effect was greatly reduced in the presence of CISE and ribavirin, a broad-spectrum antiviral agent (Figure 2A). The virus titers were significantly decreased by CISE in a dose-dependent manner (Figure 2B, IC90 = 179 μg/ml) without cytotoxicity (Figure 2C).

To determine which component in the CISE exerts antiviral effects, CISE was further separated into water (CISE-DW) or ethanol (CISE-ET) fractions as described in Figure 1. Similar to CISE, CISE-ET inhibited PEDV infection in a dose-dependent manner (Figure 2D, IC90 = 30 μg/ml) without cytotoxicity (Figure 2E). Unlike CISE and CISE-ET, CISE-DW had no effect on PEDV infection or cell viability (Figures 2F,G). These data indicated that the components in CISE-ET exhibited antiviral activity *in vitro*.

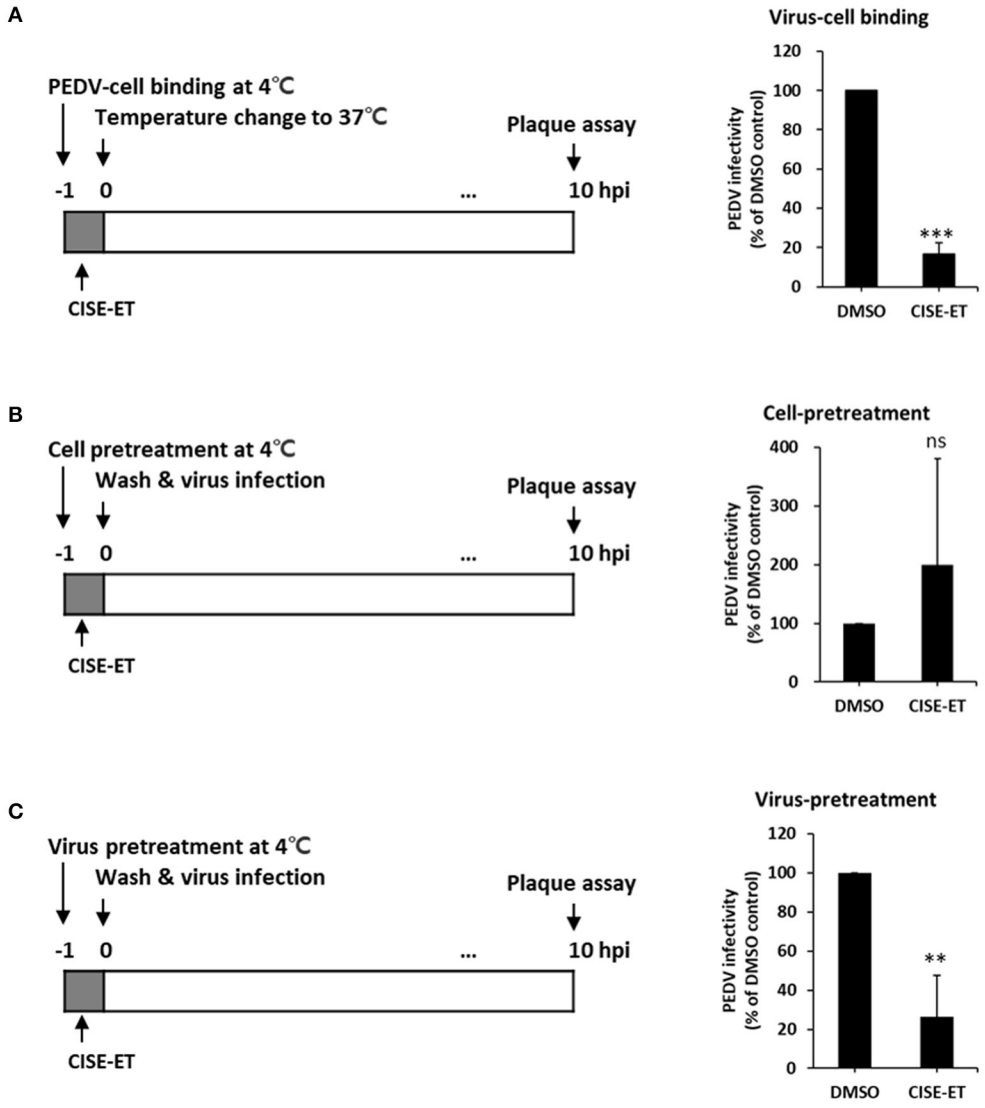

FIGURE 4
CISE-ET blocked virus–cell binding by inactivating PEDV particles. **(A)** Vero cells were infected with PEDV (MOI = 1), treated with 30 μg/ml CISE-ET at 4°C for 1 h, washed with PBS, and maintained in SFM for 10 h. **(B)** Vero cells were treated with 30 μg/ml CISE-ET at 4°C for 1 h, washed with PBS and infected with PEDV (MOI = 1) at 37°C. After 2 h, the cells were washed with PBS and maintained in SFM for 8 h. **(C)** PEDV was incubated with 30 μg/ml CISE-ET at 4°C for 1 h and then diluted in SFM 10-fold. Vero cells were then infected with diluted PEDV (MOI = 1) at 37°C for 1, washed with PBS and maintained in SFM for 8 h. At 10 hpi, the virus titers were measured by plaque assay. The viral infectivity is expressed relative to that found for the DMSO control group. The error bars represent the SDs from the means ($n = 3$). $^{**}P < 0.01$; $^{***}P < 0.001$; ns, not significant.

CISE-ET inhibited the early phase of PEDV infection

To determine the stage at which CISE-ET exerted inhibitory activity, we performed time-of-addition experiments with a concentration of 30 μg/ml (Figure 3A). More than 90% of viral infection was reduced by the administration of CISE-ET at the time of virus infection (0 h, Figure 3B, $P < 0.001$). No antiviral activity was observed when CISE-ET was added at or after 2 hpi (Figure 3B). These data indicated that CISE-ET inhibited the early phase of PEDV infection.

CISE-ET inhibited virus–Cell binding by affecting the virus

CoV entry is mediated by the interaction of S protein with cellular receptors and subsequently by membrane fusion catalyzed by host proteases (26, 27). To examine whether CISE-ET inhibited virus–cell binding, we measured the antiviral activity of CISE-ET during virus–cell binding. CISE-ET treatment during virus–cell binding showed inhibition rates of ∼80% (Figure 4A, $P < 0.001$). To further explore the mechanism through which CISE-ET inhibits virus–cell binding, we determined the antiviral activity of CISE-ET using two experiments: (i) cell pretreatment and (ii) virus pretreatment. No antiviral activity was observed when cells were pretreated with CISE-ET (Figure 4B, $P = 0.3911$). In contrast, virus pretreatment with CISE-ET resulted in inhibition rates of ∼90% (Figure 4C, $P < 0.001$). These data indicated that CISE-ET inhibited virus–cell binding, most likely by inhibiting the initial processes of virus attachment and entry.

CISE-ET inhibited virus–Cell fusion

We then examined whether CISE-ET blocks virus–cell fusion. As shown in Figure 5A, PEDV particles were allowed to first attach to the target cells at 4°C. After 1 h, unbound viruses were removed, and virus-bound cells were incubated at 37°C to initiate viral entry/fusion in the presence or absence of CISE-ET. In the absence of trypsin, the PEDV titers were significantly decreased under CISE-ET-treated conditions, similar to the results obtained with treatment with the endosomal cathepsin inhibitor E64d and treatment with the vacuolar H+ ATPase inhibitor BafA1 (Figure 5B, $P < 0.001$). These findings revealed that CISE-ET also strongly inhibited the post-attachment membrane fusion steps. The addition of exogenous trypsin increased PEDV infection in Vero cells by 10-fold and rescued PEDV infection under BafA1- and E64d-treated conditions (Figure 5B, $P = 0.015$, $P = 0.030$). Interestingly, enhancement of PEDV infection by trypsin was not observed in the presence of CISE-ET (Figure 5B, $P = 0.731$). These data indicated that CISE-ET inhibited PEDV S-mediated virus–cell fusion.

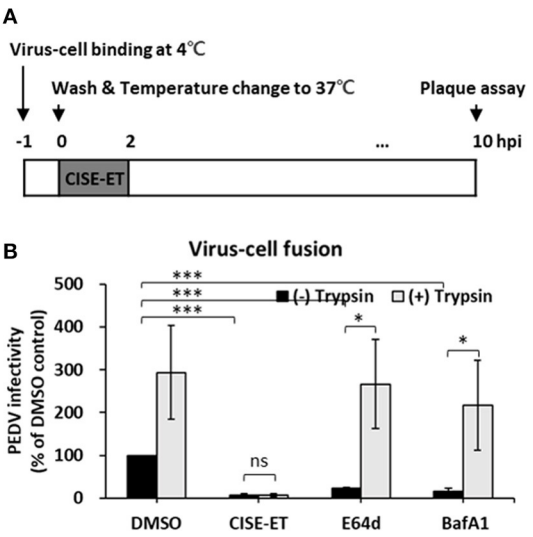

FIGURE 5
CISE-ET inhibited virus–cell fusion and proteolytic cleavage of S proteins. **(A)** Schematic of the synchronized infection experiments of virus–cell fusion. Vero cells were incubated with PEDV (MOI = 1) for 1 h at 4°C for initial binding, washed with PBS and treated with 30 μg/ml CISE-ET and/or 10 μg/ml trypsin for 2 h at 37°C. The inoculums were then removed, and the cells were maintained in SFM for 8 h. At 10 hpi, the virus titers were measured by plaque assay. **(B)** The viral infectivity is expressed relative to that found for the DMSO control group. The error bars represent the SDs from the means ($n = 3$). *$P < 0.05$; ***$P < 0.001$; ns, not significant.

CISE-ET inhibited the viral entry of MERS-CoV, SARS-CoV, and SARS-CoV-2

We subsequently sought to examine the effect of CISE on other viruses in the *Coronaviridae* family, including MERS-CoV, SARS-CoV, and SARS-CoV-2. Specifically, pseudotyped viruses expressing corresponding S proteins were generated and transduced into target cells in the presence of CISE or CISE-ET. The addition of CISE blocked the entry of MERS-CoV (Figure 6A, IC50 = 30 μg/ml) but did not affect SARS-CoV (Figure 6B) or SARS-CoV-2 (Figure 6C) pseudovirus transduction. CISE-ET treatment efficiently inhibited MERS-CoV (IC50 = 20 μg/ml, Figure 6A), SARS-CoV (IC50 = 14 μg/ml, Figure 6B), and SARS-CoV-2 (IC50 = 21 μg/ml, Figure 6C) pseudovirus transduction. VSV entry was not affected by either CISE or CISE-ET (Figure 6D). These results indicated that CISE also exhibited antiviral activity against select viruses in the *Coronaviridae* family.

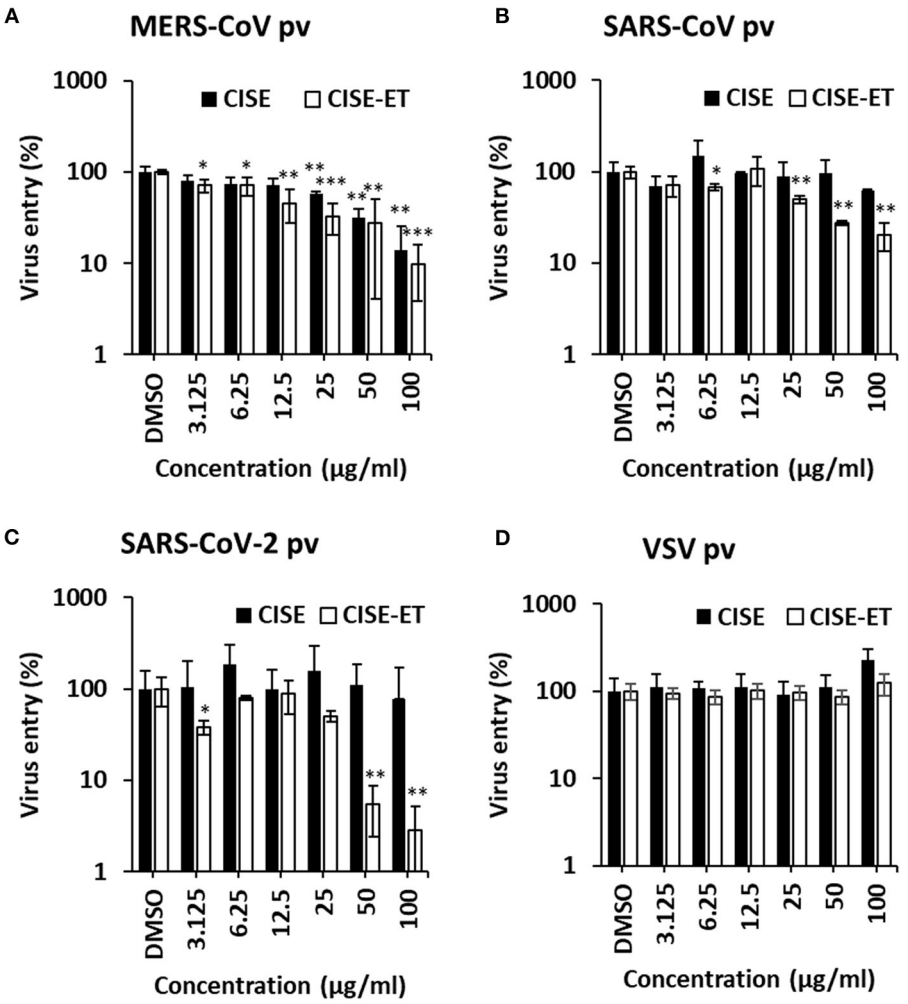

FIGURE 6
CISE-ET inhibited the entry of MERS-CoV, SARS-CoV and SARS-CoV-2. Huh7 cells were transduced with MERS-CoV **(A)**, SARS-CoV **(B)**, SARS-CoV-2 **(C)** or VSV **(D)** pseudotyped viruses (pvs) in the presence of various concentrations of CISE or CISE-ET. The viral entry was quantified by a luciferase assay at 48 h post-transduction and expressed relative to that found for the DMSO control group. The error bars represent the SDs from the means ($n = 3$). *$P < 0.05$; **$P < 0.01$; ***$P < 0.001$.

Discussion

There are currently no approved anti-PEDV therapeutics. The use of prophylactic/therapeutic treatment against PEDV may reduce the incidence of infection in endemic areas.

In an effort to develop antiviral drugs for PEDV, several naturally derived materials displaying anti-PEDV activity, including *Pogostemon cablin* polysaccharide (28), aloe (29), tomatidine (30), *Epimedium koreanum* Nakai (31), and various Vietnamese traditional medicinal plants (32), have been identified. In the present study, we demonstrated that CISE inhibits PEDV infection by targeting viral entry. CISE-ET blocked viral attachment and fusion to host cells without exerting any significant influence on viral replication or release. Our findings suggest that CIS is an important source of antiviral materials for the development of PEDV therapeutics.

Plant-derived extracts such as CISE contain numerous components, and their actions in cultured cells may be mutually exclusive. Moreover, the biological effect of natural compound extracts might be derived from the synergistic integration of multiple components with different potencies and efficacies. Gallic acid and ellagic acid are the most abundant components in CISE and exhibit antiviral activity against many viruses (20–23), and we thus speculate that these components might exert an antiviral effect. The analysis

of the components in CISE has not been fully elucidated, and the identification of the leading active component is an essential step for drug development that can offer new therapeutic options for clinical use. We are currently preparing peak-by-peak fractions to identify the active ingredients in CISE-ET and will subsequently compare the potency of their antiviral activities.

The mode of action is an unanswered question. Our data provide evidence showing that CISE-ET specifically blocks virus entry by inhibiting PEDV attachment and post-attachment viral entry/fusion. CoV cell entry is orchestrated by S proteins that bind to cellular receptors and catalyze virus–cell membrane fusion (26, 33, 34). Studies have suggested that virus–cell membrane fusion is triggered by several activators of S proteins: (i) protease cleavage at S1/S2, (ii) receptor-induced conformational changes, (iii) protease cleavage at S2', and (iv) ionic changes (26, 35–37). Along with conformational changes in S proteins, curvature of the viral envelope and cellular membrane is needed for membrane fusion to occur (38, 39). Because CISE showed specific but broad antiviral activity against the tested CoVs (Figure 6), we initially hypothesized that CISE might exert its antiviral activity by inhibiting the proteolytic cleavage of S protein. However, the proteolytic processing of PEDV S and MERS-CoV S was not affected (data not shown). Alternatively, we speculate that CISE might apply its antiviral activity by intercalating with the surface structural components of PEDV, such as S glycoproteins and the viral envelope. For instance, the drug could interfere with conformational changes in S proteins and/or curvature of the viral envelope. Further analysis is necessary to clarify the specific molecular mechanism(s) of action.

Conclusion

In conclusion, this study provides the first demonstration of the antiviral activity of CISE against PEDV and multiple CoVs. CISE impedes PEDV infection by blocking viral attachment and fusion. These findings suggest that CISE and its components could be developed as therapeutic or prophylactic agents for restricting the viral entry of selected CoVs.

Data availability statement

The original contributions presented in the study are included in the article/supplementary material, further inquiries can be directed to the corresponding authors.

Author contributions

J-EP and T-WK: conceptualized the study and prepared the manuscript and supervised the project and acquired the funding. J-EP, JK, SJ, YC, and T-WK: designed the study methodology and analyzed data. All the authors reviewed and edited the manuscript and have read and agreed to the published version of this manuscript.

Funding

This work was supported by the National Research Foundation of Korea (NRF) grant funded by the Korean government (MSIT) (2020R1C1C1012854), the Basic Science Research Program through the National Research Foundation of Korea funded by the Ministry of Education (2021R1A6A1A03045495), and the research fund of Chungnam National University.

Conflict of interest

The authors declare that the research was conducted in the absence of any commercial or financial relationships that could be construed as a potential conflict of interest.

Publisher's note

References

1. Debouck P, Pensaert M. Experimental infection of pigs with a new porcine enteric coronavirus, Cv 777. *Am J Vet Res.* (1980) 41:219–23.

2. Jung K, Wang Q, Scheuer KA, Lu Z, Zhang Y, Saif LJ. Pathology of US porcine epidemic diarrhea virus strain Pc21a in gnotobiotic pigs. *Emerg Infect Dis.* (2014) 20:662–5. doi: 10.3201/eid2004.131685

3. Madson DM, Magstadt DR, Arruda PH, Hoang H, Sun D, Bower LP, et al. Pathogenesis of porcine epidemic diarrhea virus isolate (Us/Iowa/18984/2013) in 3-week-old weaned pigs. *Vet Microbiol.* (2014) 174:60–8. doi: 10.1016/j.vetmic.2014.09.002

4. Pensaert MB, de Bouck P. A new coronavirus-like particle associated with diarrhea in swine. *Arch Virol.* (1978) 58:243–7. doi: 10.1007/BF01317606

5. Takahashi K, Okada K, Ohshima K. An outbreak of swine diarrhea of a new-type associated with coronavirus-like particles in Japan. *Nihon Juigaku Zasshi.* (1983) 45:829–32. doi: 10.1292/jvms1939.45.829

6. Stevenson GW, Hoang H, Schwartz KJ, Burrough ER, Sun D, Madson D, et al. Emergence of porcine epidemic diarrhea virus in the United States: clinical signs, lesions, and viral genomic sequences. *J Vet Diagn Invest.* (2013) 25:649–54. doi: 10.1177/1040638713501675

7. Cima G. Fighting a deadly pig disease. Industry, veterinarians trying to contain ped virus, new to the US. *J Am Vet Med Assoc.* (2013) 243:469–70. doi: 10.2460/javma.243.4.458

8. Jung K, Saif LJ, Wang Q. Porcine epidemic diarrhea virus (Pedv): an update on etiology, transmission, pathogenesis, and prevention and control. *Virus Res.* (2020) 286:198045. doi: 10.1016/j.virusres.2020.198045

9. Lee C. Porcine epidemic diarrhea virus: an emerging and re-emerging epizootic swine virus. *Virol J.* (2015) 12:193. doi: 10.1186/s12985-015-0421-2

10. Shibata I, Tsuda T, Mori M, Ono M, Sueyoshi M, Uruno K. Isolation of porcine epidemic diarrhea virus in porcine cell cultures and experimental infection of pigs of different ages. *Vet Microbiol.* (2000) 72:173–82. doi: 10.1016/S0378-1135(99)00199-6

11. Jung BS, Lee NK, Na DS Yu HH, Paik HD. Comparative analysis of the antioxidant and anticancer activities of chestnut inner shell extracts prepared with various solvents. *J Sci Food Agric.* (2016) 96:2097–102. doi: 10.1002/jsfa.7324

12. Noh JR, Gang GT, Kim YH, Yang KJ, Hwang JH, Lee HS, et al. Antioxidant effects of the chestnut (castanea crenata) inner shell extract in T-Bhp-Treated Hepg2 Cells, and Ccl4- and high-fat diet-treated mice. *Food Chem Toxicol.* (2010) 48:3177–83. doi: 10.1016/j.fct.2010.08.018

13. Kim KM, Lee HS, Yun MK, Cho HY Yu HJ, Sohn J, et al. Fermented castanea crenata inner shell extract increases fat metabolism and decreases obesity in high-fat diet-induced obese mice. *J Med Food.* (2019) 22:264–70. doi: 10.1089/jmf.2018.4240

14. Noh JR, Kim YH, Gang GT, Hwang JH, Lee HS, Ly SY, et al. Hepatoprotective effects of chestnut (castanea crenata) inner shell extract against chronic ethanol-induced oxidative stress in C57bl/6 mice. *Food Chem Toxicol.* (2011) 49:1537–43. doi: 10.1016/j.fct.2011.03.045

15. Chi YS, Heo MY, Chung JH, Jo BK, Kim HP. Effects of the chestnut inner shell extract on the expression of adhesion molecules, fibronectin and vitronectin, of skin fibroblasts in culture. *Arch Pharm Res.* (2002) 25:469–74. doi: 10.1007/BF02976604

16. Tsurunaga Y, Takahashi T. Evaluation of the antioxidant activity, deodorizing effect, and antibacterial activity of 'porotan' chestnut by-products and establishment of a compound paper. *Foods.* (2021) 10:1141. doi: 10.3390/foods10051141

17. Cho DY, Ko HM, Kim J, Kim BW, Yun YS, Park JI, et al. Scoparone inhibits Lps-simulated inflammatory response by suppressing Irf3 and Erk in Bv-2 microglial cells. *Molecules.* (2016) 21:1718. doi: 10.3390/molecules21121718

18. Jeong CH, Choi GN, Kim JH, Kwak JH, Choi SG, Heo HJ. Characterization of antioxidant activities from chestnut inner skin extracts. *Food Sci Biotechnol.* (2009) 18:1218–23.

19. SoN KH, Yang HE, Lee SC, Chung JH, Jo BK, Kim HP, et al. Antioxidative Activity of the Extract from the Inner Shell of Chestnut. *J Appl Pharm.* (2005) 13:150–5.

20. Park SW, Kwon MJ, Yoo JY, Choi HJ, Ahn YJ. Antiviral activity and possible mode of action of ellagic acid identified in lagerstroemia speciosa leaves toward human rhinoviruses. *BMC Complement Altern Med.* (2014) 14:171. doi: 10.1186/1472-6882-14-171

21. Cui Q, Du R, Anantpadma M, Schafer A, Hou L, Tian J, et al. Identification of ellagic acid from plant Rhodiola Rosea L. as an anti-ebola virus entry inhibitor. *Viruses.* (2018) 10:152. doi: 10.3390/v10040152

22. Morosetti G, Criscuolo AA, Santi F, Perno CF, Piccione E, Ciotti M. Ellagic acid and annona muricata in the chemoprevention of Hpv-related pre-neoplastic lesions of the cervix. *Oncol Lett.* (2017) 13:1880–4. doi: 10.3892/ol.2017.5634

23. Chen GH, Lin YL, Hsu WL, Hsieh SK, Tzen JTC. Significant elevation of antiviral activity of strictinin from pu'er tea after thermal degradation to ellagic acid and gallic acid. *J Food Drug Anal.* (2015) 23:116–23. doi: 10.1016/j.jfda.2014.07.007

24. Hofmann M, Wyler R. Propagation of the virus of porcine epidemic diarrhea in cell culture. *J Clin Microbiol.* (1988) 26:2235–9. doi: 10.1128/jcm.26.11.2235-2239.1988

25. Lee SR, Jo SL, Heo JH, Kim TW, Lee KP, Hong EJ. The aqueous fraction of castanea crenata inner shell extract reduces obesity and intramuscular lipid accumulation *via* induction of mitochondrial respiration and fatty acid oxidation in muscle. *Phytomedicine.* (2022) 98:153974. doi: 10.1016/j.phymed.2022.153974

26. Belouzard S, Millet JK, Licitra BN, Whittaker GR. Mechanisms of coronavirus cell entry mediated by the viral spike protein. *Viruses.* (2012) 4:1011–33. doi: 10.3390/v4061011

27. Millet JK, Whittaker GR. Host cell proteases: critical determinants of coronavirus tropism and pathogenesis. *Virus Res.* (2015) 202:120–34. doi: 10.1016/j.virusres.2014.11.021

28. Chen Y, Luo Q, Li S, Li C, Liao S, Yang X, et al. Antiviral activity against porcine epidemic diarrhea virus of pogostemon cablin polysaccharide. *J Ethnopharmacol.* (2020) 259:113009. doi: 10.1016/j.jep.2020.113009

29. Xu Z, Liu Y, Peng P, Liu Y, Huang M, Ma Y, et al. Aloe extract inhibits porcine epidemic diarrhea virus *in vitro* and *in vivo*. *Vet Microbiol.* (2020) 249:108849. doi: 10.1016/j.vetmic.2020.108849

30. Wang P, Bai J, Liu X, Wang M, Wang X, Jiang P. Tomatidine inhibits porcine epidemic diarrhea virus replication by targeting 3cl protease. *Vet Res.* (2020) 51:136. doi: 10.1186/s13567-020-00865-y

31. Cho WK, Kim H, Choi YJ, Yim NH, Yang HJ, Ma JY. Epimedium koreanum nakai water extract exhibits antiviral activity against porcine epidermic diarrhea virus *in vitro* and *in vivo*. *Evid Based Complement Alternat Med.* (2012) 2012:985151. doi: 10.1155/2012/985151

32. Trinh TBN, Le DH, Nguyen TTK, Nguyen VT, Nguyen MH, Muller M, et al. *In vitro* antiviral activities of ethanol and aqueous extracts of Vietnamese traditional medicinal plants against porcine epidemic diarrhea virus: a coronavirus family member. *Virusdisease.* (2021) 32:797–803. doi: 10.1007/s13337-021-00709-z

33. Matsuyama S, Ujike M, Morikawa S, Tashiro M, Taguchi F. Protease-mediated enhancement of severe acute respiratory syndrome coronavirus infection. *Proc Natl Acad Sci U S A.* (2005) 102:12543–7. doi: 10.1073/pnas.0503203102

34. Nash TC, Buchmeier MJ. Entry of mouse hepatitis virus into cells by endosomal and nonendosomal pathways. *Virology.* (1997) 233:1–8. doi: 10.1006/viro.1997.8609

35. Millet JK, Whittaker GR. Physiological and molecular triggers for Sars-Cov membrane fusion and entry into host cells. *Virology.* (2018) 517:3–8. doi: 10.1016/j.virol.2017.12.015

36. Matsuyama S, Taguchi F. Receptor-induced conformational changes of murine coronavirus spike protein. *J Virol.* (2002) 76:11819–26. doi: 10.1128/JVI.76.23.11819-11826.2002

37. Lai AL, Millet JK, Daniel S, Freed JH, Whittaker GR. The Sars-Cov fusion peptide forms an extended bipartite fusion platform that perturbs membrane order in a calcium-dependent manner. *J Mol Biol.* (2017) 429:3875–92. doi: 10.1016/j.jmb.2017.10.017

38. Chernomordik LV, Kozlov MM. Protein-lipid interplay in fusion and fission of biological membranes. *Annu Rev Biochem.* (2003) 72:175–207. doi: 10.1146/annurev.biochem.72.121801.161504

39. Yuan L, Zhang S, Wang Y, Li Y, Wang X, Yang Q. Surfactin inhibits membrane fusion during invasion of epithelial cells by enveloped viruses. *J Virol.* (2018) 92:e00809–18. doi: 10.1128/JVI.00809-18